# *Chapter: 4*

# Structural Characterization and High Temperature Dielectric Studies on off-Stoichiometric 0.38BMW-0.62PT Ceramics

## 4.1 Introduction

The stoichiometric $ABO_3$ perovskite piezoelectric ceramics consist a class of materials that achieve both scientific and industrial importance [Jaffe et al. (1971), Pandey et al. (2014), Upadhyay et al. (2015)] as well as various device applications [Bellaiche et al. (2000), Stringer et al. (2005)]. Conventionally deviation from stoichiometry of the ceramic samples has been treated as a demerit and most of the efforts are done to control the stoichiometry of the samples during synthesis [Kofstad (1972); Smyth (2000); Moulson and Herbert (2003)]. In recent years, researchers have deliberately introduced off-stoichiometry in several ceramic systems and interesting improvement in the physical properties has been reported to appear [Kang et al. (2013), Li et al. (2016), Mishra et al. (2019)]. Recently off-stoichiometric samples of several ferroelectric solid solutions have been investigated [Kang et al. (2013), Mishra et al (2019)]. It has been found that the deviation from the stoichiometry has significant impact on the crystal structure, microstructure and phase transition behaviour and ferroelectric/piezoelectric properties of the samples [Kang et al. (2013)]. Kang et al. [2013] have investigated the effect of adding excess PbO, $Bi_2O_3$, NiO and $TiO_2$ on the microstructure and electrical properties of $0.45PbTiO_3$-$0.55Bi(Ni_{1/2}Ti_{1/2})O_3$ ceramic. It has been found that the addition of excess PbO and NiO modifies the crystal structure of the samples. The problem of leakage current is decreased by doping of excess reactants while excess $TiO_2$ decreases the coercive field [Kang et al. (2013)]. The grain size and the density of the excess PbO doped samples were observed to increase significantly. Similarly in case of $Na_{1/2}Bi_{1/2}TiO_3$ ceramic, excess of Bi affects the microstructure and electrical properties significantly [Zhong et al. (2006), Li et al. (2016)]. Further, in $Na_{0.5}Bi_{0.5}TiO_3$ and $0.94Na_{0.5}Bi_{0.5}TiO_3$-$0.06BaTiO_3$ ceramics, Mishra et al. [2019] have reported that grain size, polarization, crystal structure,

piezoelectric response and electrical resistivity is significantly modified by off-stoichiometry of the sodium and bismuth ions. Thus deliberate introduction of off-stoichiometry in ferroelectric and piezoelectric ceramics has significant potential for controlling the crystal structure, microstructure and physical properties. As discussed in Chapter 2, the compositions of (1-x)$Bi(Mg_{3/4}W_{1/4})O_3$-x$PbTiO_3$ with lower $PbTiO_3$ concentration have small amount of impurity phases because of less stable perovskite phase of $Bi(Mg_{3/4}W_{1/4})O_3$, having small tolerance factor. To eliminate the appearance of impurity phases during synthesis in lead based perovskites like (1-x)$Pb(Mg_{1/3}Nb_{2/3})O_3$-x$PbTiO_3$ and (1-x)$Pb(Zn_{1/3}Nb_{2/3})O_3$-x$PbTiO_3$, excess amount of reactant oxides have been used by several research groups [Shrout and Swartz (1983), Goo et al. (1986), Koyuncu and Pilgrim (1999), Wang and Schulze (1990), Swartz et al. (1984), Joy and Sreedhar (1997) ]. Addition of excess MgO and PbO has been found to be effective in reducing the formation of impurities during synthesis of (1-x)$Pb(Mg_{1/3}Nb_{2/3})O_3$-x$PbTiO_3$ and (1-x)$Pb(Zn_{1/3}Nb_{2/3})O_3$-x$PbTiO_3$ ceramics [Wang and Schulze (1990), Swartz et al. (1984), Joy and Sreedhar (1997)]. In view of this, it will also be interesting to investigate the effect of excess addition of reactant oxides during synthesis of (1-x)$Bi(Mg_{3/4}W_{1/4})O_3$-x$PbTiO_3$. As discussed in section 3.5.3 of Chapter 3, the XPS studies of the (1-x)$Bi(Mg_{3/4}W_{1/4})O_3$-x$PbTiO_3$ samples suggest that tungsten ion has both the +6 and +5 ionization states. The reduction of the valence of the tungsten from the ideal +6 valance for B-site of the designed perovskite structure will affect the electro-neutrality of the samples. To compensate for the reduced valance of tungsten from +6 to +5, addition of excess amount of reactants may be helpful. In view of the foregoing, we have investigated how the off-stoichiometry affects the crystal structure, microstructure, dielectric behiavour and phase transition of (1-x)$Bi(Mg_{3/4}W_{1/4})O_3$-x$PbTiO_3$ ceramics.

This chapter presents the results of our investigation on the crystal structure, microstructure, dielectric and phase transition behaviour of non-stoichiometric $0.38Bi(Mg_{3/4}W_{1/4})O_3$-$0.62PbTiO_3$ ceramic prepared by adding 1, 2, 3 and 5 mol% of excess PbO, $Bi_2O_3$, MgO, $H_2WO_4$ and $TiO_2$. It is observed that excess of PbO and $TiO_2$ have significantly impact on the crystal structure, microstructure and dielectric behaviour of the samples.

## 4.2 Experimental Details

The off-stoichiometric samples of $0.38Bi(Mg_{3/4}W_{1/4})O_3$-$0.62PbTiO_3$ ceramics have been prepared by solid state ceramic method described in chapter 2. Different compositions of off-stoichiometric samples were synthesized by mixing of the reactants, with 1, 2, 3 and 5 mol% excess of PbO, $Bi_2O_3$, MgO, $H_2WO_4$ and $TiO_2$. As described in Chapter 2, the required amounts of analytical reagent grade reactant powders for various compositions were properly hand mixed in a mortar with the help of pestle and then the mixture was ball milled for 6 hrs with acetone as mixing medium using an agate jar and zirconia balls. The ball-milled mixture was dried at room temperature in open air and then calcination process was carried out in alumina crucible inside muffle furnace at an optimized temperature of 850 ºC for 6 hrs. The phase purity of the calcined samples was checked by recording X-ray diffraction (XRD) patterns using Miniflex 600 (Rigaku, Japan) X-ray diffractometer. The XRD data was collected in the 2θ range 10º to 100° at a scan rate of 1°/min with scan step of 0.02°. The aqueous solution of 2% PVA (polyvinyl alcohol) was used as a binder for the pellet formation. The PVA solution was properly mixed and pellets was formed by using 12 mm diameter steel die with the help of a uniaxial hydraulic press at an optimized load of 75 kN. The PVA binder was burned out from the green pellets by firing at 500 °C for 12

hrs and the samples were sintered at optimized temperature of 990 °C for 3 hrs. The pellet densities were measured using Archimedes principle and more than 97% were obtained after sintering. The sintered pellets were crushed in fine powders using motor pestle and then annealed at 500 °C for 12 hours to remove the strain introduced during crushing. The XRD data were collected on annealed powders. The microstructure of the sintered pellets was studied by scanning electron microscopy (SEM) using Zeiss (Evo Research 18). The flat surfaces of the sintered pellets were electroded by silver paste for dielectric characterization. After applying silver paste, the pellets were first dried at ~ 150 °C in an oven and then fired at 500 °C for 30 minutes. Temperature-dependent dielectric measurements were carried out using Impedance Analyzer (Keysight E4990A) at the heating rate of 2 $^{o}$C/min at various frequencies. The structural analysis of all the samples was carried out by the Rietveld method using FullProf Suite [Carvajal 2011].

### 4.3 Results and Discussion

#### 4.3.1 Effect of PbO off-stoichiometry on the Room Temperature Crystal Structure of 0.38BMW-0.62PT Ceramic

**Fig. 4.1** shows room temperature powder XRD patterns of sintered samples of 0.38BMW-0.62PT ceramics along with 1, 2, 3 and 5 mol% excess of PbO. As discussed in Chapter 3, the room temperature crystal structure of the stoichiometric 0.38BMW-0.62PT ceramic has the coexistence of cubic (*Fm*-3*m* space group) and tetragonal (*I*4/*m* space group). Because of this phase coexistence the pseudocubic (200) XRD profile around 46$^{o}$ appears as a triplet. As discussed in Chapter 2, the middle peak corresponds to the cubic phase while side peaks are due to the tetragonal phases. A careful examination of the XRD profile around 46$^{o}$ for the off-stoichiometric 0.38BMW-0.62PT samples with excess PbO reveals that these compositions also have the

coexistence of the cubic and tetragonal structures. However, increasing excess of PbO results in decreased intensity of the (111) superlattice reflection appearing due to B-site cationic ordering. For 5 mol % excess of PbO, the superlattice reflection completely vanishes which reveals that the B-site cationic ordering is not present in this compositions. Thus the structure for this composition is coexisting disordered cubic (space group *Pm*-3*m*) and tetragonal (space group *P*4*mm*) phases. Further, the intensity of the (200) peak corresponding to the cubic phase is seen to be significantly enhanced for the higher PbO concentration (see peak around $46^{o}$). This suggests that the phase fraction of the cubic phase increases with excess PbO addition. In contrast to this, the tetragonal structure is observed to be stabilized for $0.45PbTiO_3$-$0.55Bi(Ni_{1/2}Ti_{1/2})O_3$ ceramic doped with excess PbO [Kang et al 2013]. Moreover, the intensity of the XRD peaks corresponding to the $Bi_2WO_6$ impurity phase also decreases with increasing excess amounts of PbO. The reduction of the impurity phases by adding excess PbO is already reported in MPB ceramics like $(1-x)Pb(Mg_{1/3}Nb_{2/3})O_3$-$xPbTiO_3$ and $(1-x)Pb(Zn_{1/3}Nb_{2/3})O_3$-$xPbTiO_3$ [Wang and Schulze (1990), Swartz et al. (1984), Joy and Sreedhar (1997)]. The crystal structure of the non-stoichiometric samples with 1, 2, 3 and 5 mol% excess PbO has been refined using Rietveld structural analysis. The phase fraction of the ordered cubic structure (*Fm*-3*m*) increases and phase fraction of the ordered tetragonal phase (*I*4*/m*) decreases with increasing excess doping concentration of PbO. The Rietveld fits for the XRD patterns of stoichiometric 0.38BMW-0.62PT and 5 mole % excess PbO samples are shown in **Fig. 4.2**. As can be seen from this figure, the fits are quite good confirming our considered crystal structures. Rietveld refined structural parameters for stoichiometric and 5 mol % excess PbO samples is listed in **Table 4.1**.

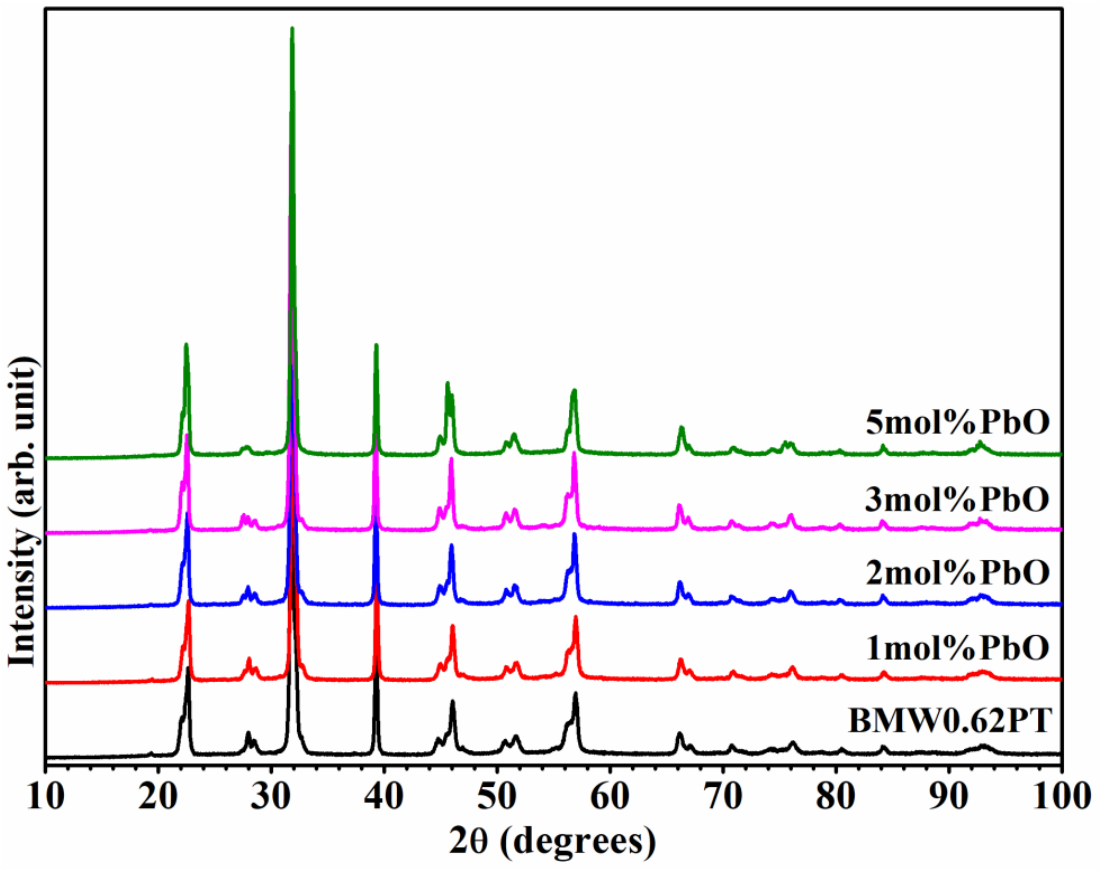


**Figure 4.1** Powder XRD patterns of $0.38Bi(Mg_{3/4}W_{1/4})O_3$-$0.62PbTiO_3$ ceramics having 1, 2, 3 and 5 mol% excess amount of PbO. The lower pattern is for stoichiometric sample.

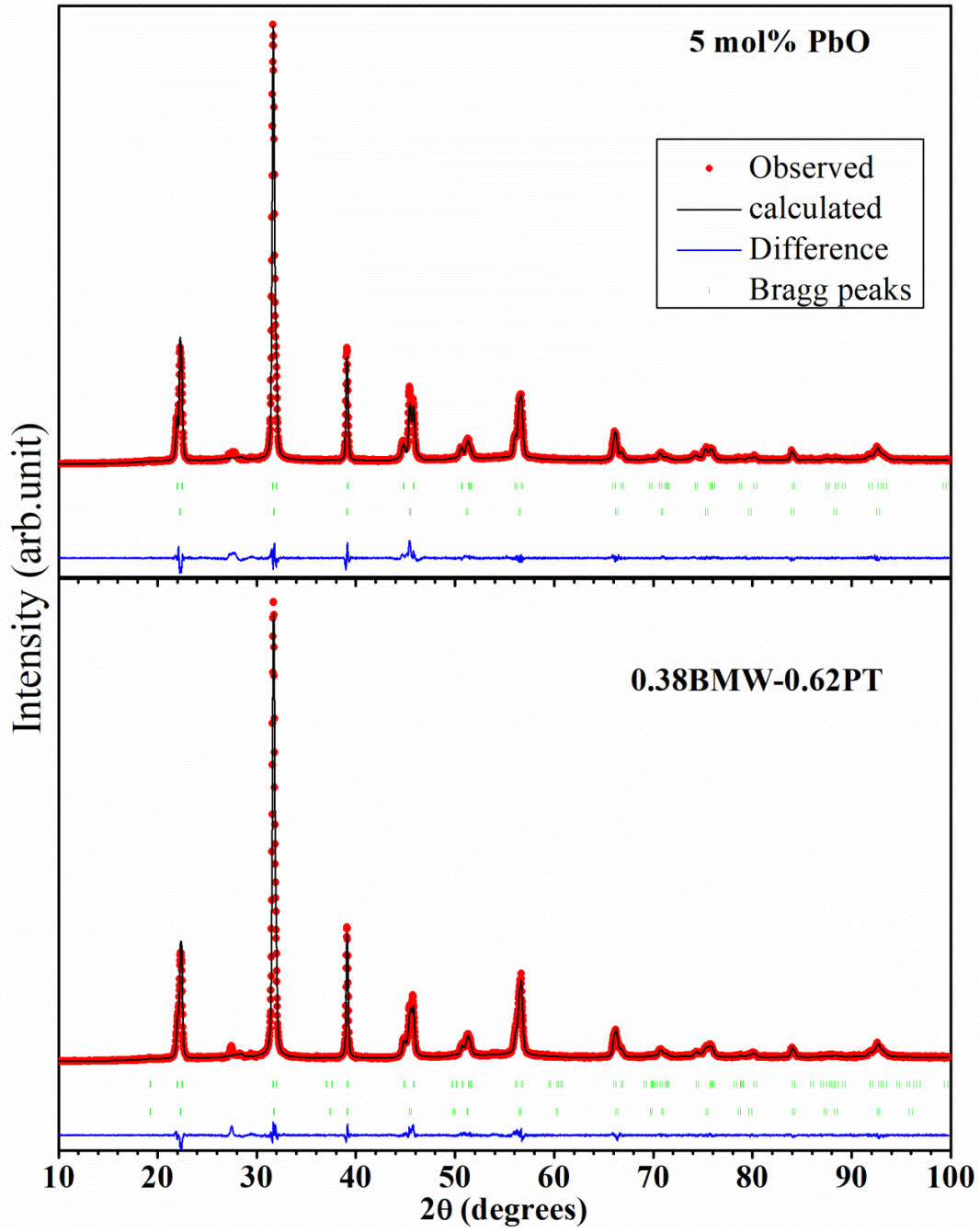


**Figure 4.2** Experimentally observed (red dots), Rietveld calculated (overlapping black line) and their difference (continuous blue curve) XRD profiles for stoichiometric $0.38Bi(Mg_{3/4}W_{1/4})O_3$-$0.62PbTiO_3$ (lower panel) and with excess of 5 mol% PbO (upper panel), obtained after Rietveld structural analysis. The stoichiometric sample has coexisting cubic (*Fm*-3*m)* and tetragonal (*I*4/*m*) structures while 5 mol% excess PbO sample has coexisting cubic (P*m*-3*m)* and tetragonal (*P*4*mm*) structures, respectively. The vertical bars upper (tetragonal), lower (cubic) above the difference plot show the peak positions.

**Table 4.1**: Rietveld refined structural parameters of 0.38BMW-0.62PT for stoichiometric and 5 mole % excess PbO samples.

| 0.38BMW-0.62PT (*Fm*-3*m*), % Fraction=14.57, $\chi^2$ =2.95, $R_{wp}$ = 10.6 | | | | |
|---|---|---|---|---|
| Elements | X | y | z | B |
| Pb | 0.250 | 0.250 | 0.250 | 1.780 (1) |
| Bi | 0.250 | 0.250 | 0.250 | 0.000 (0) |
| Mg | 0.500 | 0.500 | 0.500 | 0.000 |
| W | 0.000 | 0.000 | 0.000 | 2.702 |
| Ti1 | 0.500 | 0.500 | 0.500 | 3.592 |
| Ti2 | 0.000 | 0.000 | 0.000 | 0.000(0) |
| O | 0.251(5) | 0.000 | 0.000 | 3.738 |
| 0.38BMW-0.62PT (*I*4/*m*), % Fraction =85.43, $\chi^2$ =2.95, $R_{wp}$ = 10.6 | | | | |
| Pb | 0.000 | 0.500 | 0.250 | 4.460(2) |
| Bi | 0.000 | 0.500 | 0.250 | 4.424(2) |
| Mg | 0.000 | 0.000 | 0.500 | 9.362(8) |
| W | 0.000 | 0.000 | 0.000 | 9.362(8) |
| Ti1 | 0.000 | 0.000 | 0.500 | 0.003(1) |
| Ti2 | 0.000 | 0.000 | 0.000 | 0.000 |
| O1 | 0.000 | 0.000 | 0.23913(5) | 9.703(9) |
| O2 | 0.250 | 0.250 | 0.000 | 2.593(2) |
| 5mol% excess PbO (*Fm*-3*m*), % Fraction =56.56, $\chi^2$ =2.02, $R_{wp}$= 8.52 | | | | |
| Pb | 0.250 | 0.250 | 0.250 | 5.014(7) |
| Bi | 0.250 | 0.250 | 0.250 | 5.014(7) |
| Mg | 0.500 | 0.500 | 0.500 | 0.500(1) |
| W | 0.000 | 0.000 | 0.000 | 0.00 |
| Ti1 | 0.500 | 0.500 | 0.500 | 0.00 |
| Ti2 | 0.000 | 0.000 | 0.000 | 0.194(2) |
| O | 0.252(5) | 0.000 | 0.000 | 0.000 |
| 5mol% excess PbO (*P*4*mm*), % Fraction =43.44, $\chi^2$ =2.02, $R_{wp}$ = 8.52 | | | | |
| Pb | 0.000 | 0.000 | 0.000 | 3.460(2) |
| Bi | 0.000 | 0.000 | 0.000 | 3.428(2) |
| Mg | 0.500 | 0.500 | 0.5534(3) | 0.362(3) |
| W | 0.500 | 0.500 | 0.5534(3) | 0.362(1) |
| Ti | 0.500 | 0.500 | 0.5534(3) | 0.000 |
| O1 | 0.500 | 0.500 | 0.0885(8) | 0.703(9) |
| O2 | 0.500 | 0.000 | 0.000 | 0.259(2) |

### 4.3.2 Effect of $Bi_2O_3$ off-stoichiometry on the Room Temperature Crystal Structure of 0.38BMW-0.62PT Ceramic

**Fig. 4.3** shows the room temperature powder XRD patterns of 0.38BMW-0.62PT ceramics chemically modified by adding 1, 2, 3 and 5 mol% excess of $Bi_2O_3$ sintered at 990 $^oC$ for 3 hrs. For comparison, lower pattern for the stoichiometric samples is also given. The nature of the x-ray diffraction profiles for all the compositions is almost similar, which suggests that there is no significant structural modification due to off-stoichiometry of $Bi_2O_3$. The crystal structure for the chemically modified 0.38BMW-0.62PT ceramics with excess $Bi_2O_3$ also exhibit coexistence of the ordered cubic (*Fm*-3*m*) and ordered tetragonal (*I*4/*m*) structures. In contrast to this, the tetragonal structure is observed to be stabilized for $0.45PbTiO_3$-$0.55Bi(Ni_{1/2}Ti_{1/2})O_3$ ceramic doped with excess $Bi_2O_3$ [Kang et al. 2013]. Further, in contrast to the excess PbO samples, there is no significant change in the intensity of the XRD peaks for the impurity phase with increasing excess amount of $Bi_2O_3$.

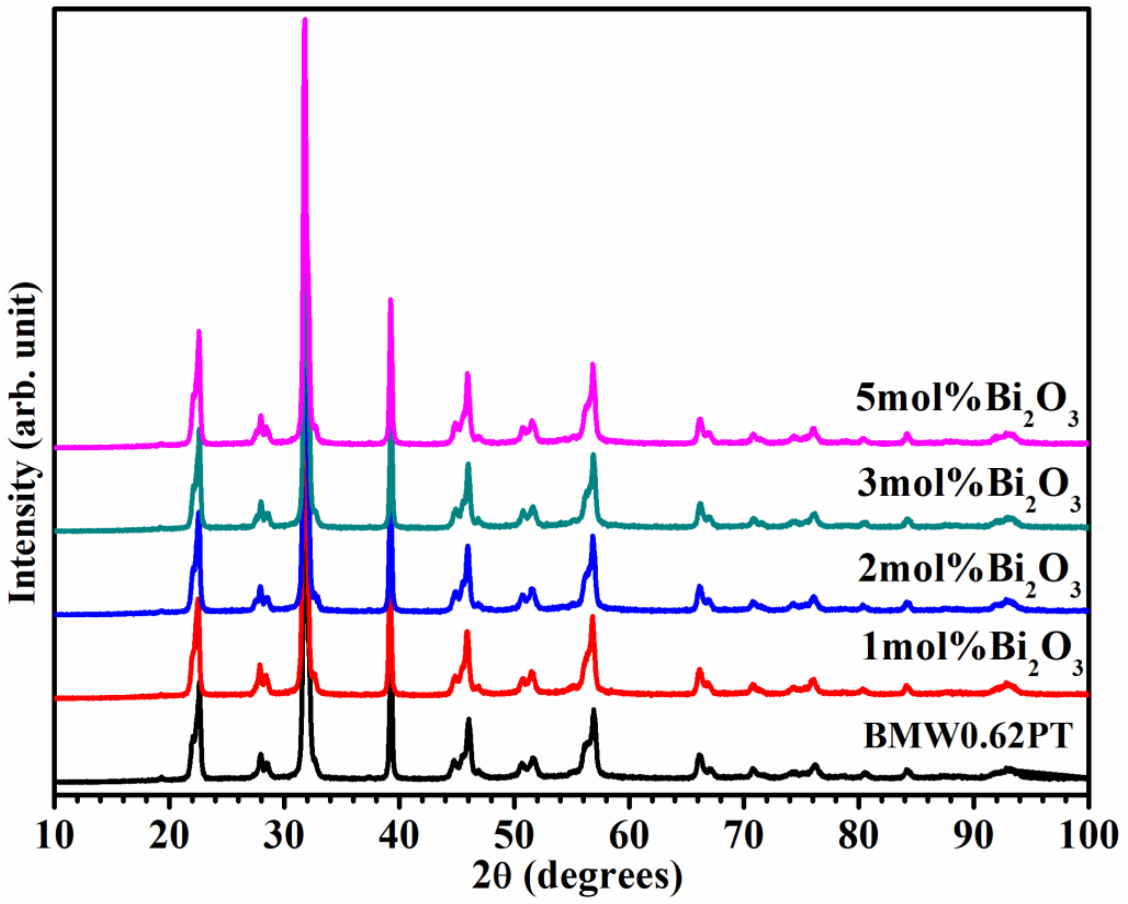


**Figure 4.3** Powder XRD patterns of $0.38Bi(Mg_{3/4}W_{1/4})O_3$-$0.62PbTiO_3$ ceramics modified with 1, 2, 3 and 5 mol% excess amount of $Bi_2O_3$ sintered at 990 ºC.

Rietveld structure refinement of $0.38Bi(Mg_{3/4}W_{1/4})O_3$-$0.62PbTiO_3$ samples with excess $Bi_2O_3$ confirms the coexistence of ordered cubic structure with *Fm*-3*m* space group and ordered tetragonal structure with *I4/m* space group for all the concentrations. **Fig. 4.4** shows the Rietveld fit for the $0.38Bi(Mg_{3/4}W_{1/4})O_3$-$0.62PbTiO_3$ sample with 5 mole% excess $Bi_2O_3$. The fit is quite satisfactory.

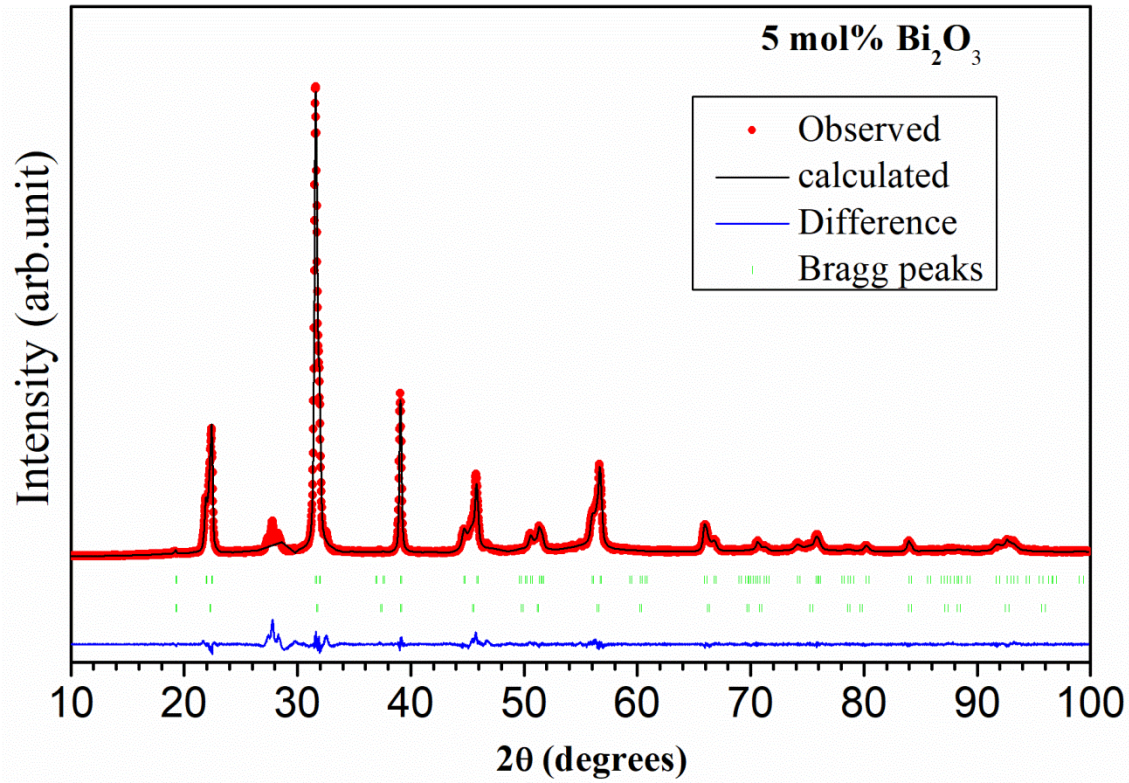


**Figure 4.4** Experimentally observed (red dots), Rietveld calculated (overlapping black line) and their difference (continuous blue curve) XRD profiles for $0.38Bi(Mg_{3/4}W_{1/4})O_3$-$0.62PbTiO_3$ with 5 mol% excess $Bi_2O_3$, obtained after Rietveld structural analysis using coexisting Cubic (*Fm*-3*m*) and tetragonal (*I*4/*m*) structures. The vertical bars upper (tetragonal), lower (cubic) above the difference plot show the peak positions.

### 4.3.3 Effect of $TiO_2$ off-stoichiometry on the Room Temperature Crystal Structure of 0.38BMW-0.62PT Ceramic

**Fig. 4.5** shows room temperature powder XRD patterns for sintered ceramic samples of 0.38BMW-0.62PT having excess 1, 2, 3 and 5 mol% of $TiO_2$. The effect of excess $TiO_2$ on the crystal structure of the off-stoichiometric samples is exactly opposite to that observed for the samples with PbO off-stoichiometry. The intensity of the superlattice reflection due to B-site cationic ordering significantly increases with increasing $TiO_2$ excess concentration. Examination of the pseudocubic (200) XRD

profile triplet around 46° reveals that the peaks due to tetragonal phase become stronger and clearly splitted with increasing excess $TiO_2$ concentration (see **Fig. 4.5**). Thus, the addition of excess amount of $TiO_2$ in 0.38BMW-0.62PT is stabilizing the tetragonal structure and also strengthening the B-site cationic ordering. In contrasts to the PbO excess samples, the intensity of the XRD peaks due to impurity phase increases with increasing excess amounts of $TiO_2$.

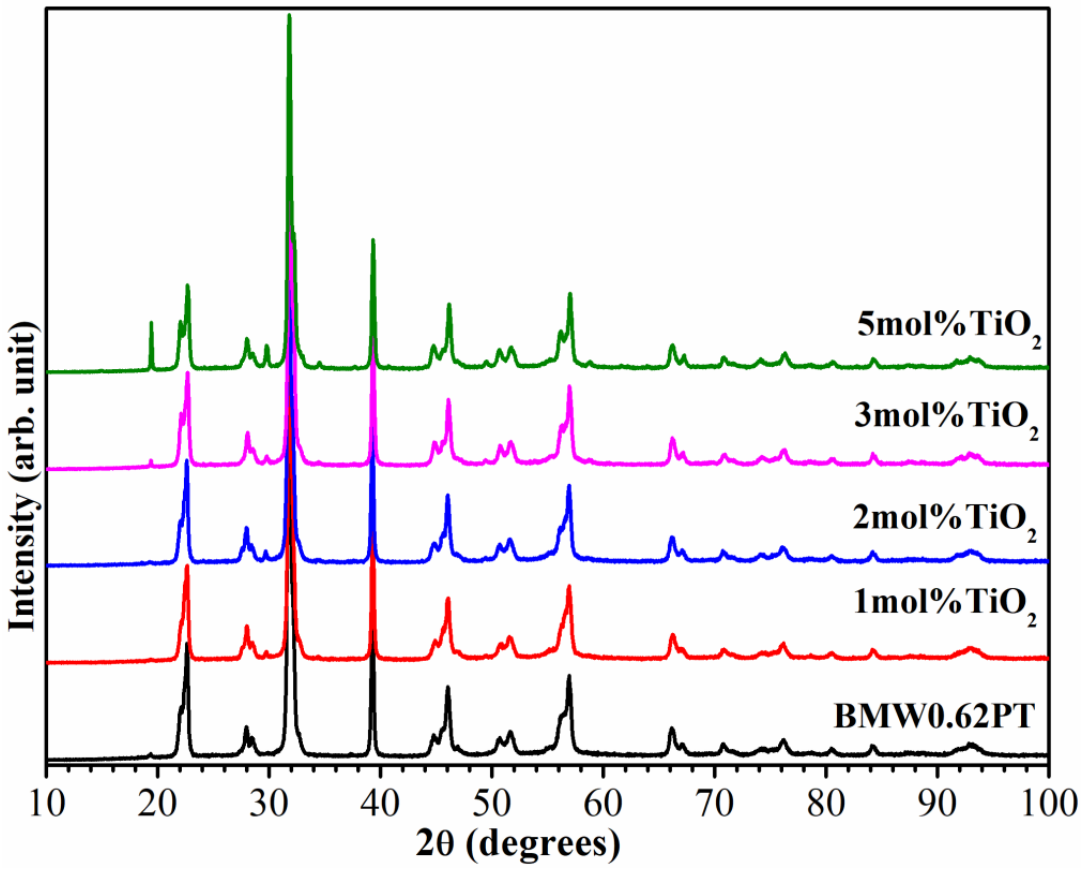


**Figure 4.5** Powder XRD patterns of $0.38Bi(Mg_{3/4}W_{1/4})O_3$-$0.62PbTiO_3$ ceramics chemically modified with 1, 2, 3 and 5 mol% excess amount of $TiO_2$ sintered at 990 °C.

Rietveld fit for the $0.38Bi(Mg_{3/4}W_{1/4})O_3$-$0.62PbTiO_3$ sample with 5 mole% excess $TiO_2$ is shown in **Fig. 4.6.** Excluding the impurity peaks, all the peaks for the perovskite phase are accounted well by considering coexisting order cubic (*Fm*-3*m*) and

ordered tetragonal (*I4/m*) structures. Mismatch in the intensity of some of the diffraction profiles results due to off-stoichiometry of the sample.

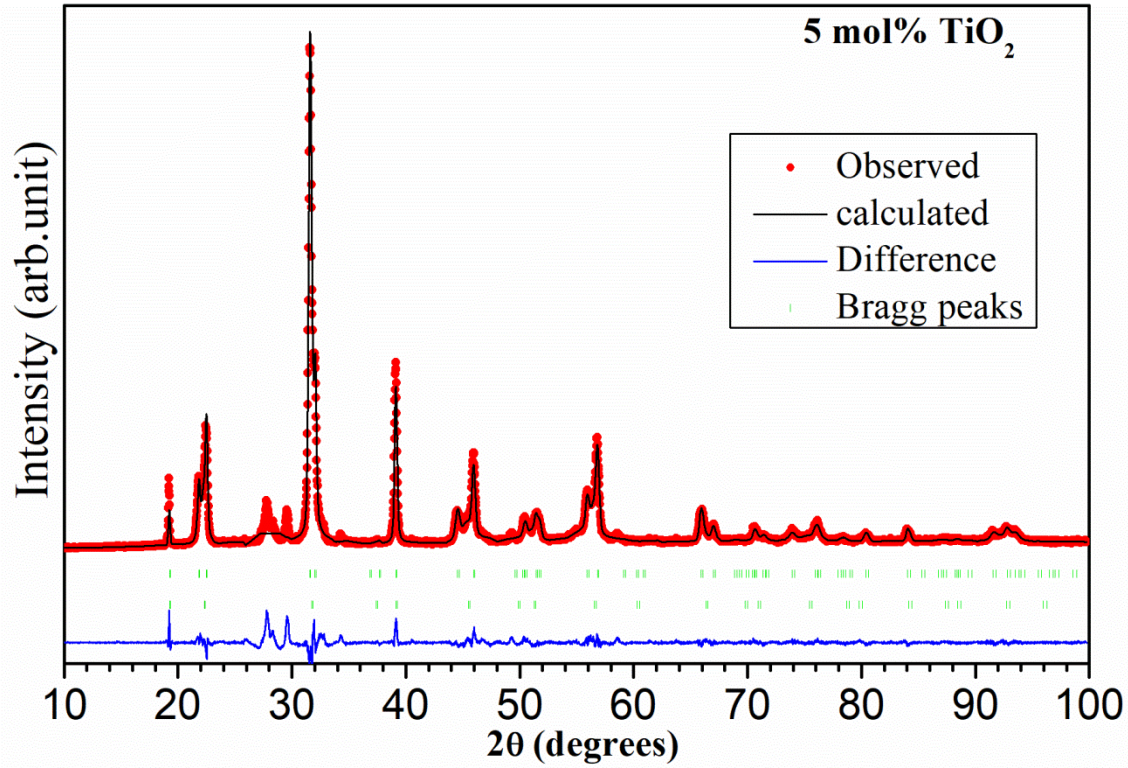


**Figure 4.6** Experimentally observed (red dots), Rietveld calculated (overlapping black line) and their difference (continuous blue curve) XRD profiles for $0.38Bi(Mg_{3/4}W_{1/4})O_3$-$0.62PbTiO_3$ with 5mol% excess of $TiO_2$ obtained after Rietveld structural analysis using coexisting cubic (*Fm*-3*m*) and tetragonal (*I4/m*) structures. The vertical bars upper (tetragonal), lower (cubic) above the difference plot show the peak positions.

### 4.3.4 Effect of $H_2WO_4$ off-stoichiometry on the Room Temperature Crystal Structure of 0.38BMW-0.62PT Ceramic

**Fig. 4.7** shows room temperature powder XRD patterns of sintered samples of 0.38BMW-0.62PT ceramics chemically modified by adding 1, 2, 3 and 5 mol% excess of $H_2WO_4$. Similar to the 0.38BMW-0.62PT samples with $Bi_2O_3$ off-stoichiometry

discussed in section 4.3.2, addition of excess $H_2WO_4$ does not have significant effect on the crystal structure as well as the phase fraction of $Bi_2WO_6$ impurity phase. As shown in **Fig. 4.7**, the XRD patterns of all the compositions with $H_2WO_4$ excess is nearly similar. Rietveld structure refinement confirms that the crystal structures of chemically modified 0.38BMW-0.62PT ceramics with excess $H_2WO_4$ also have the coexistence of the ordered cubic and ordered tetragonal structures similar to stoichiometric 0.38BMW-0.62PT sample.

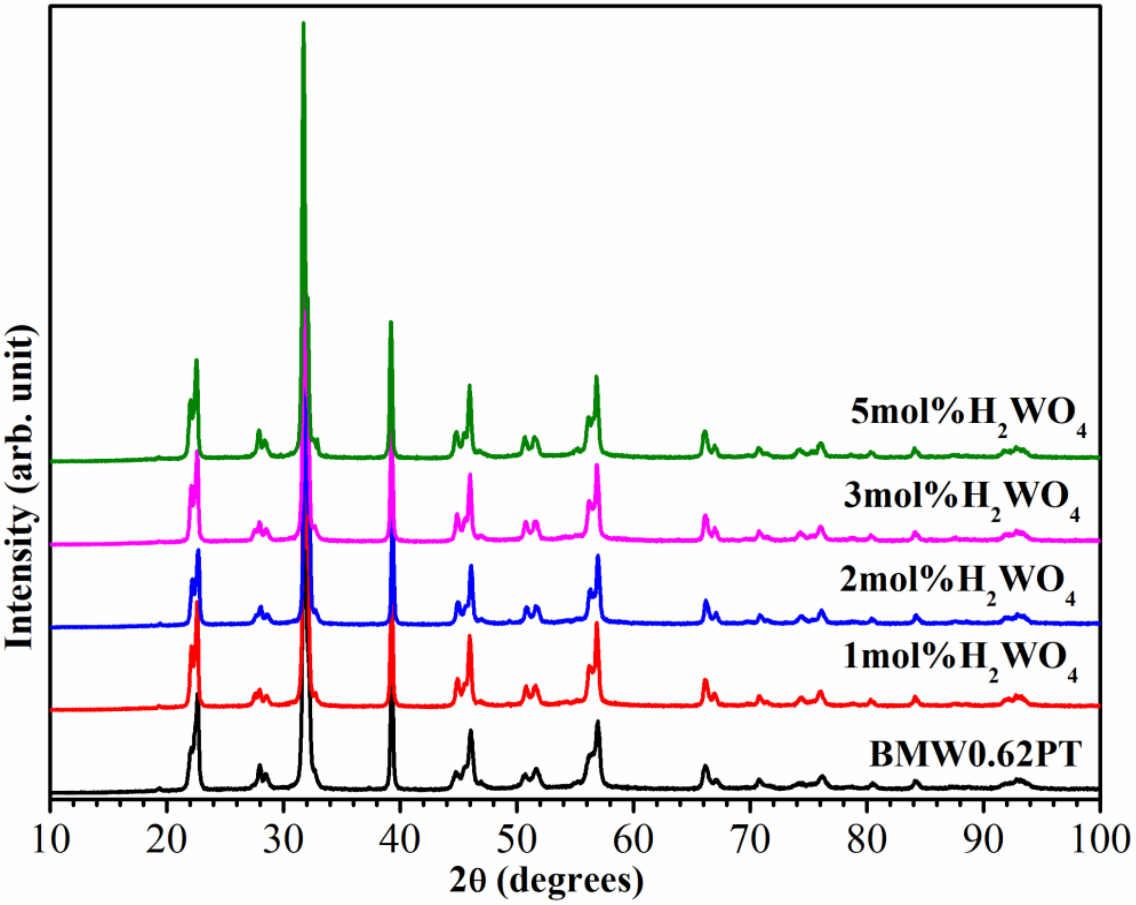


**Figure 4.7** Powder XRD patterns of $0.38Bi(Mg_{3/4}W_{1/4})O_3$-$0.62PbTiO_3$ ceramic samples chemically modified with 1, 2, 3 and 5 mol% excess amount of $H_2WO_4$ sintered at 990 $^oC$. The lower pattern is for the stoichiometric sample.

Rietveld fit for the XRD pattern of 5 mol% excess amount of $H_2WO_4$ sample considering ordered cubic structure with *Fm*-3*m* space group and ordered tetragonal structure with *I*4/*m* space group is shown in **Fig. 4.8** which is quite good.

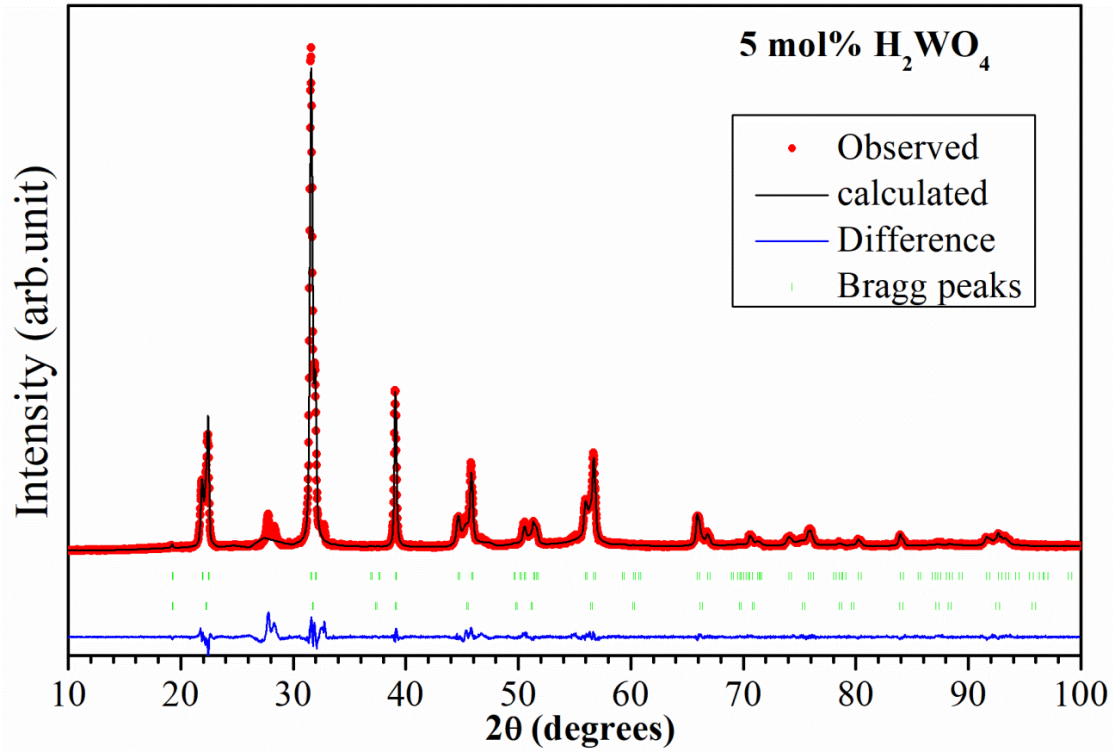


**Figure 4.8** Experimentally observed (red dots), Rietveld calculated (overlapping black line) and their difference (continuous blue curve) XRD profiles for $0.38Bi(Mg_{3/4}W_{1/4})O_3$-$0.62PbTiO_3$ with excess of 5mol% $H_2WO_4$, obtained after Rietveld structural analysis using coexisting cubic (*Fm*-3*m*) and tetragonal (*I*4/*m*) structures. The vertical bars upper (tetragonal), lower (cubic) above the difference plot show the peak positions.

### 4.3.5 Effect of MgO off-stoichiometry on the Room Temperature Crystal Structure of 0.38BMW-0.62PT Ceramic

**Fig. 4.9** shows the room temperature powder XRD patterns of 0.38BMW-0.62PT ceramics chemically modified by adding 1, 2, 3 and 5 mol% excess of MgO. Similar to the 0.38BMW-0.62PT samples with $Bi_2O_3$ and $H_2WO_4$ off-stoichiometry,

addition of excess amount of MgO does not have any significant impact on the crystal structure. There is no significant effect on the presence of $Bi_2WO_6$ impurity phase also. In contrast, adding excess amount of MgO is reported to be very effective in decreasing the formation of impurity phases in MPB ceramics like (1-x)Pb($Mg_{1/3}Nb_{2/3}$)$O_3$-x$PbTiO_3$ and (1-x)Pb($Zn_{1/3}Nb_{2/3}$)$O_3$-x$PbTiO_3$ [Wang and Schulze (1990), Swartz et al. (1984), Joy and Sreedhar (1997)]. The crystal structure of the MgO off-stoichiometric 0.38BMW-0.62PT samples also exhibit coexistence of the ordered cubic and ordered tetragonal structures similar to stoichiometric sample.

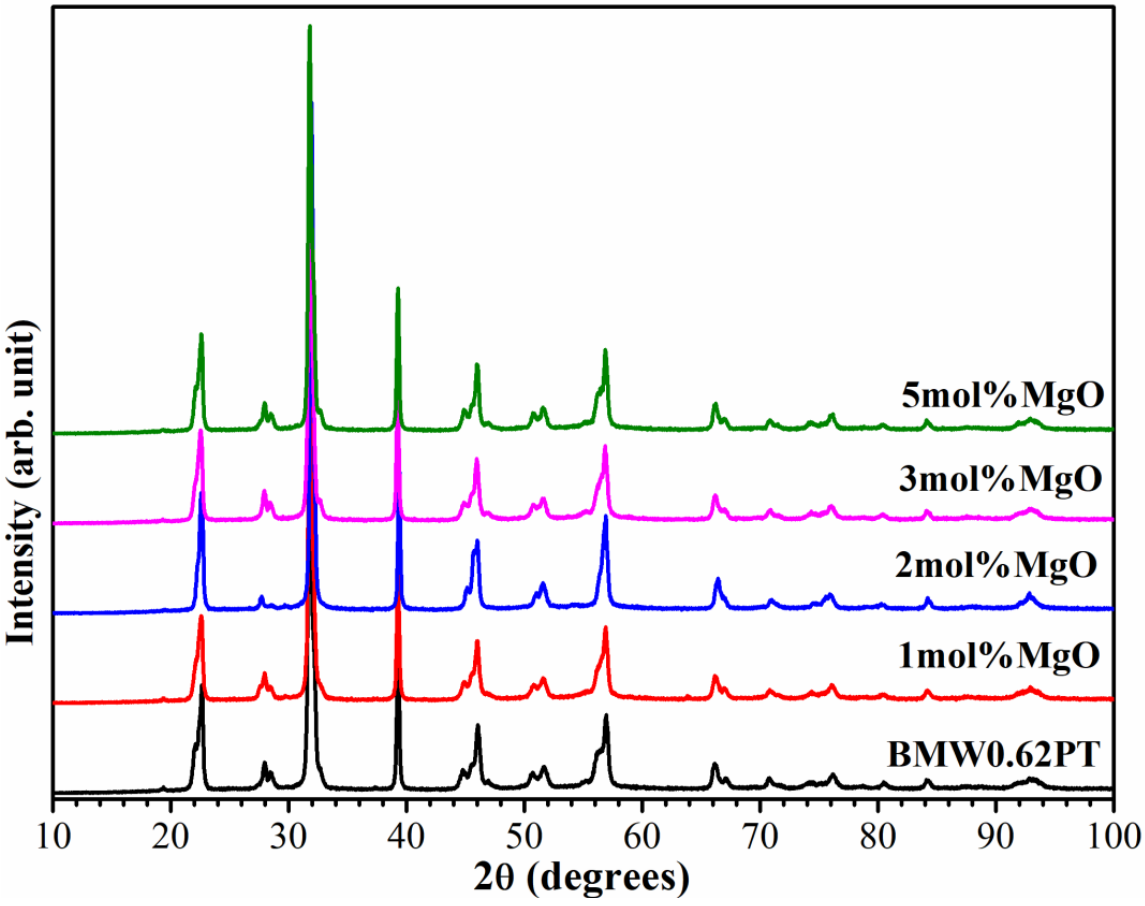


**Figure 4.9** Powder XRD patterns of 0.38Bi($Mg_{3/4}W_{1/4}$)$O_3$-0.62$PbTiO_3$ ceramics modified with 1, 2, 3 and 5 mol% excess amount of MgO sintered at 990 ºC.

The Rietveld fit for the XRD of 0.38Bi($Mg_{3/4}W_{1/4}$)$O_3$-0.62$PbTiO_3$ with excess of 5mol% MgO, obtained after structure refinement using coexisting cubic (*Fm*-3*m*) and tetragonal (*I4/m*) phases is shown in **Fig. 4.10**. The fit is quite good confirming the considered structural model.

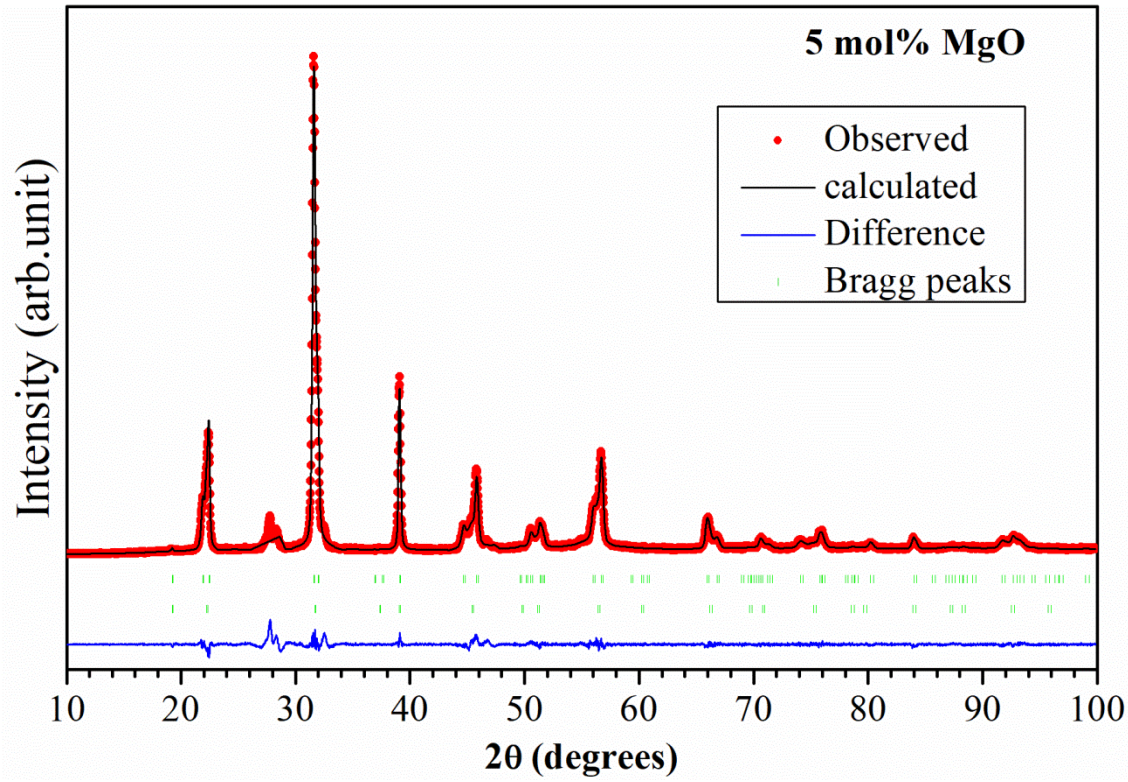


**Figure 4.10** Experimetnally observed (red dots), Rietveld calculated (overlapping black line) and their difference (continuous blue curve) XRD profiles for 0.38Bi($Mg_{3/4}W_{1/4}$)$O_3$-0.62$PbTiO_3$ with excess of 5mol% MgO, obtained after Rietveld structural analysis using coexisting cubic (*Fm*-3*m*) and tetragonal (*I4/m*) structures. The vertical bars upper (tetragonal), lower (cubic) above the difference plot show the peak positions.

### 4.3.6 Effect of off-stoichiometry on the Lattice Parameters of $0.38Bi(Mg_{3/4}W_{1/4})O_3$-$0.62PbTiO_3$ Ceramic

**Fig. 4.11** shows the variation of the lattice parameters, unit cell volume and tetragonality for 0.38BMW0.62PT ceramic chemically modified by 1, 2, 3 and 5 mol% excess of $Bi_2O_3$, $TiO_2$, PbO, $H_2WO_4$ and MgO. **Table 4.2** list the lattice parameters of off-stoichiometric 0.38BMW0.62PT ceramics chemically modified by 1, 2, 3 and 5 mol% excess of PbO, $Bi_2O_3$, MgO, $H_2WO_4$ and $TiO_2$ respectively. The lattice parameters and unit cell volume change uniformly with doping concentrations except for the MgO which shows discontinuous variation. Tetragonality increases significantly with increasing excess of $TiO_2$ concentrations. In case of PbO, the tetragonality increases first and then shows a decreasing trend. For $Bi_2O_3$, $H_2WO_4$ and MgO excess, the tetragonality increases first and then levels off at higher concentrations. It is expected that smaller concentrations are getting incorporated at the lattice/interstitials sites while higher concentrations may get segregated near grain boundaries or form impurity phases. More studies will be needed in future to exactly understand the mechanism of structural modifications due to off-stoichiometry in 0.38BMW-0.62PT.

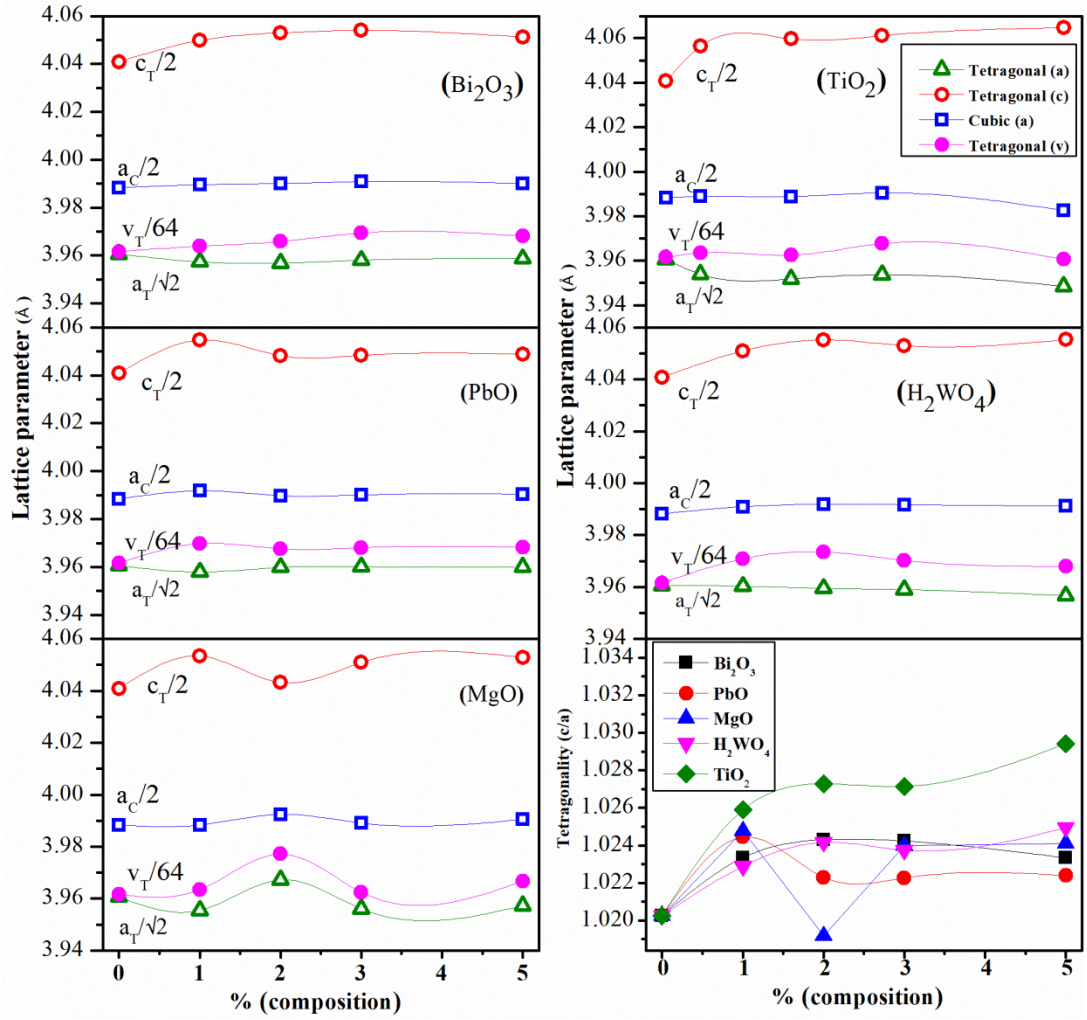


**Figure 4.11** Variation of the lattice parameters, unit cell volume and tetragonality for 0.38BMW0.62PT ceramic chemically modified by 1, 2, 3 and 5 mol% excess of $Bi_2O_3$, $TiO_2$, PbO, $H_2WO_4$ and MgO.

**Table 4.2:** Lattice parameters of off-stoichiometric 0.38BMW0.62PT ceramic chemically modified by 1, 2, 3 and 5 mol% excess of PbO, $Bi_2O_3$, MgO, $H_2WO_4$ and $TiO_2$ respectively.

| Composition | | $a_T$ | $c_T$ | $a_c$ |
|---|---|---|---|---|
| 0.38BMW0.62PT | | 5.59837(4) | 8.0954(1) | 7.97478(8) |
| PbO | 1mol% | 5.60338(2) | 8.08244(4) | 7.97478(3) |
| | 2mol% | 5.60485(3) | 8.07419(5) | 7.97478(6) |
| | 3mol% | 5.60282(6) | 8.08193(7) | 7.97478(4) |
| | 5mol% | 5.61719(2) | 8.05834(3) | 7.97478(7) |
| $Bi_2O_3$ | 1mol% | 5.60348(3) | 8.06862(2) | 7.96421(4) |
| | 2mol% | 5.60338(5) | 8.07794(1) | 7.96174(3) |
| | 3mol% | 5.60447(4) | 8.07943(3) | 7.96834(5) |
| | 5mol% | 5.60554(1) | 8.07634(2) | 7.96915(8) |
| MgO | 1mol% | 5.60377(2) | 8.07434(1) | 7.97478(1) |
| | 2mol% | 5.61721(4) | 8.05086(2) | 7.97478(3) |
| | 3mol% | 5.60449(2) | 8.07197(3) | 7.97478(2) |
| | 5mol% | 5.60146(1) | 8.07718(1) | 7.97478(1) |
| $H_2WO_4$ | 1mol% | 5.60263(2) | 8.08806(5) | 7.97478(2) |
| | 2mol% | 5.60185(3) | 8.09629(1) | 7.97478(4) |
| | 3mol% | 5.60027(9) | 8.09404(3) | 7.97478(1) |
| | 5mol% | 5.59765(8) | 8.09931(1) | 7.97478(3) |
| $TiO_2$ | 1mol% | 5.60255(7) | 8.07365(3) | 7.97709(1) |
| | 2mol% | 5.59911(1) | 8.09423(5) | 7.99435(2) |
| | 3mol% | 5.59808(7) | 8.09996(3) | 7.98562(4) |
| | 5mol% | 5.58749(5) | 8.11981(2) | 7.98562(1) |

### 4.3.7 Microstructure of $0.38Bi(Mg_{3/4}W_{1/4})O_3$-$0.62PbTiO_3$ Ceramic with off-Stoichiometry

**Fig. 4.12** shows scanning electron microscopic (SEM) images for off-stoichiometric 0.38BMW-0.62PT ceramics chemically modified with 5 mol% excess of $Bi_2O_3$, MgO, $H_2WO_4$, PbO and $TiO_2$. For comparison, the microstructure of the stoichiometric 0.38BMW-0.62PT is also shown in **Fig. 4.12** (top left image). The analysis of the SEM images reveals that the grain size of the off-stoichiometric 0.38BMW-0.62PT, after the chemical modification by 5mol % excess of $Bi_2O_3$, MgO and $H_2WO_4$, remains almost similar to that of the stoichiometric 0.38BMW-0.62PT

sample. However, the grain size for the excess PbO modified 0.38BMW-0.62PT ceramic increases significantly (6μm to 8μm). Thus the excess PbO is promoting the grain growth in off-stoichiometric sample. Similar enhancement of the grain size by PbO excess is reported for $0.45PbTiO_3$-$0.55Bi(Ni_{1/2}Ti_{1/2})O_3$ ceramic also [Kang et al. 2013]. Just opposite to PbO excess sample, the grain size is observed to be significantly lower in the excess $TiO_2$ modified sample than that for the stoichiometric one. Thus the excess $TiO_2$ acts as grain growth inhibitor.

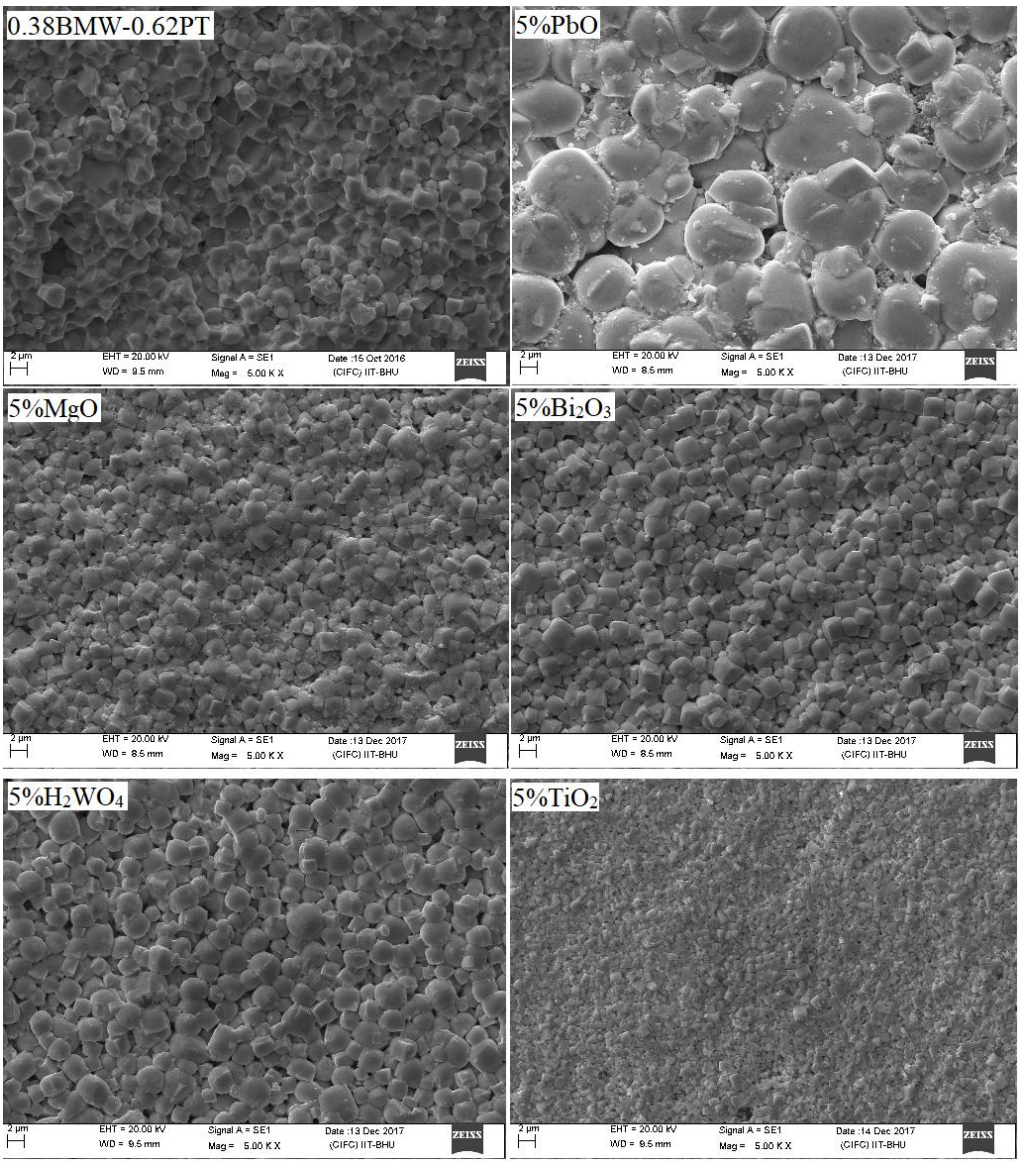


**Figure 4.12** SEM micrographs of 0.38BMW-0.62PT and modified with 5 mol% of $Bi_2O_3$, MgO, $H_2WO_4$, PbO and $TiO_2$.

**Fig. 4.13** shows the EDS spectrum of stoichiometric 0.38BMW-0.62PT and chemically modified with 5 mol% of $Bi_2O_3$, MgO, $H_2WO_4$, PbO and $TiO_2$ samples. The appearance of the characteristic peaks of the constituent elements confirms the presence of these elements. No other element is detected in the sample.

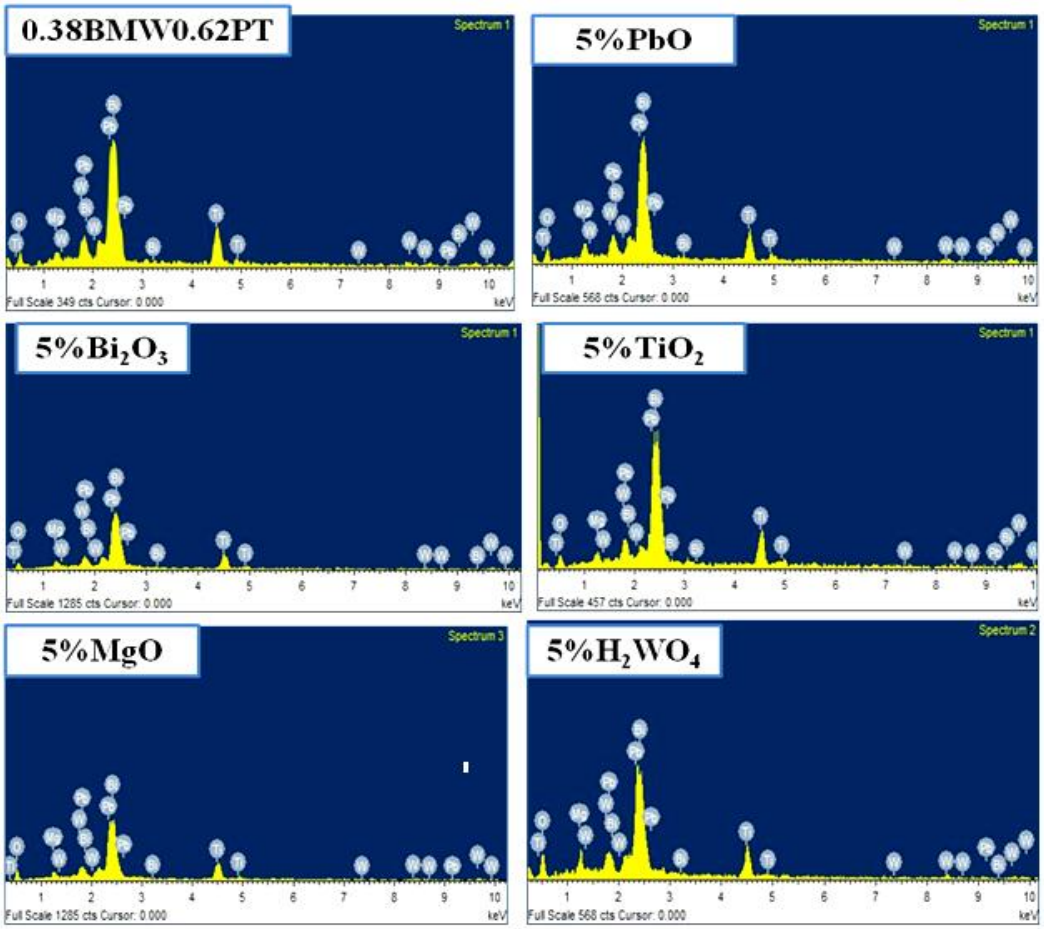


**Figure 4.13** EDS spectrum of stoichiometric 0.38BMW-0.62PT and chemically modified with 5 mol% excess of $Bi_2O_3$, MgO, $H_2WO_4$, PbO and $TiO_2$.

### 4.3.8 Temperature Dependent Dielectric Studies

To study the nature of phase transitions in chemically modified 0.38BMW-0.62PT ceramics with excess of 1, 2, 3 and 5 mol% $Bi_2O_3$, MgO, $H_2WO_4$, PbO and $TiO_2$, we have performed temperature dependent dielectric measurements at various frequencies ranging from 100 KHz to 2MHz. **Fig. 4.14** shows the temperature dependent dielectric

permittivity of stoichiometric 0.38BMW-0.62PT and that modified with 5 mol% excess of $Bi_2O_3$, MgO, $H_2WO_4$, PbO and $TiO_2$ at various frequencies. It is evident from **Fig. 4.14** that for all the compositions, dielectric behaviour and nature of phase transitions are similar to that discussed in Chapter 3 for stoichiometric samples. All the compositions show two dielectric anomalies at higher temperatures. As discussed in Chapter 3, the first anomaly is due to the structural phase transition and second anomaly appears due to the defect ordering of B-site cations and vacancies. The temperature of these dielectric anomalies is found to be slightly modified for off-stoichiometric samples. The permittivity value of the dielectric anomaly peaks are also seen to be modified due to off-stoichiometry.

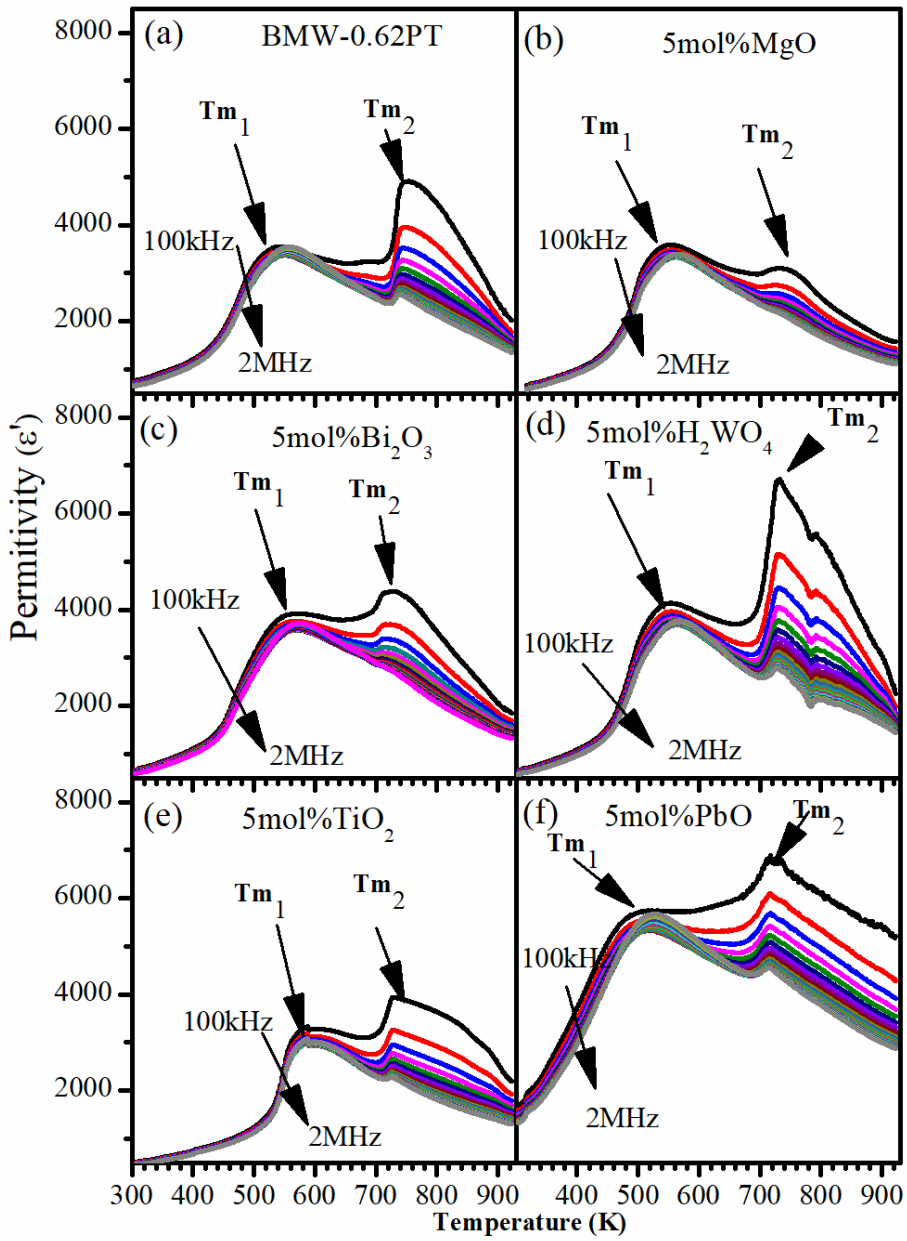


**Figure 4.14** Temperature dependent dielectric permittivity of stoichiometric 0.38BMW-0.62PT and chemically modified with 5 mol% excess of $Bi_2O_3$, MgO, $H_2WO_4$, PbO and $TiO_2$ at various frequencies.

**Table 4.3** lists the dielectric anomaly temperatures and peak permittivity value at $Tm_1$ for stoichiometric and chemically modified with 5 mol% excess of $Bi_2O_3$, MgO, $H_2WO_4$, PbO and $TiO_2$ $TiO_2$ samples measured at 1 kHz. The temperature dependent dielectric loss recorded at various frequencies for the off-stoichiometric samples with 5 mol% excess of $Bi_2O_3$, MgO, $H_2WO_4$, PbO and $TiO_2$ is shown in **Fig. 4.15** along with

that for the stoichiometric sample. The temperature dependence of dielectric loss is almost similar for all the compositions.

**Table 4.3:** Dielectric anomaly temperatures and peak permittivity value at $Tm_1$ for stoichiometric and chemically modified with 5 mol% excess of $Bi_2O_3$, MgO, $H_2WO_4$, PbO and $TiO_2$ $TiO_2$ samples measured at 1 kHz.

| Composition | | $Tm_1$ (K) | $Tm_2$ (K) | Dielectric permittivity at $Tm_1$ |
|---|---|---|---|---|
| 0.38BMW0.62PT | | 555 | 731 | **2971** |
| PbO | 1mol% | 564 | 717 | 3979 |
| | 2mol% | 560 | 712 | 4051 |
| | 3mol% | 548 | 710 | 3499 |
| | 5mol% | 522 | 718 | **5745** |
| $Bi_2O_3$ | 1mol% | 561 | 731 | 3592 |
| | 2mol% | 571 | 734 | 3532 |
| | 3mol% | 567 | 729 | 3323 |
| | 5mol% | 568 | 732 | **3919** |
| MgO | 1mol% | 569 | 721 | 3166 |
| | 2mol% | 545 | 688 | 3555 |
| | 3mol% | 562 | 739 | 3335 |
| | 5mol% | 554 | 729 | **3590** |
| $H_2WO_4$ | 1mol% | 545 | 715 | 3585 |
| | 2mol% | 601 | 713 | 3541 |
| | 3mol% | 601 | 723 | 4005 |
| | 5mol% | 556 | 732 | **4134** |
| $TiO_2$ | 1mol% | 592 | 731 | 2830 |
| | 2mol% | 602 | 730 | 3143 |
| | 3mol% | 570 | 730 | 3291 |
| | 5mol% | 603 | 720 | **3282** |

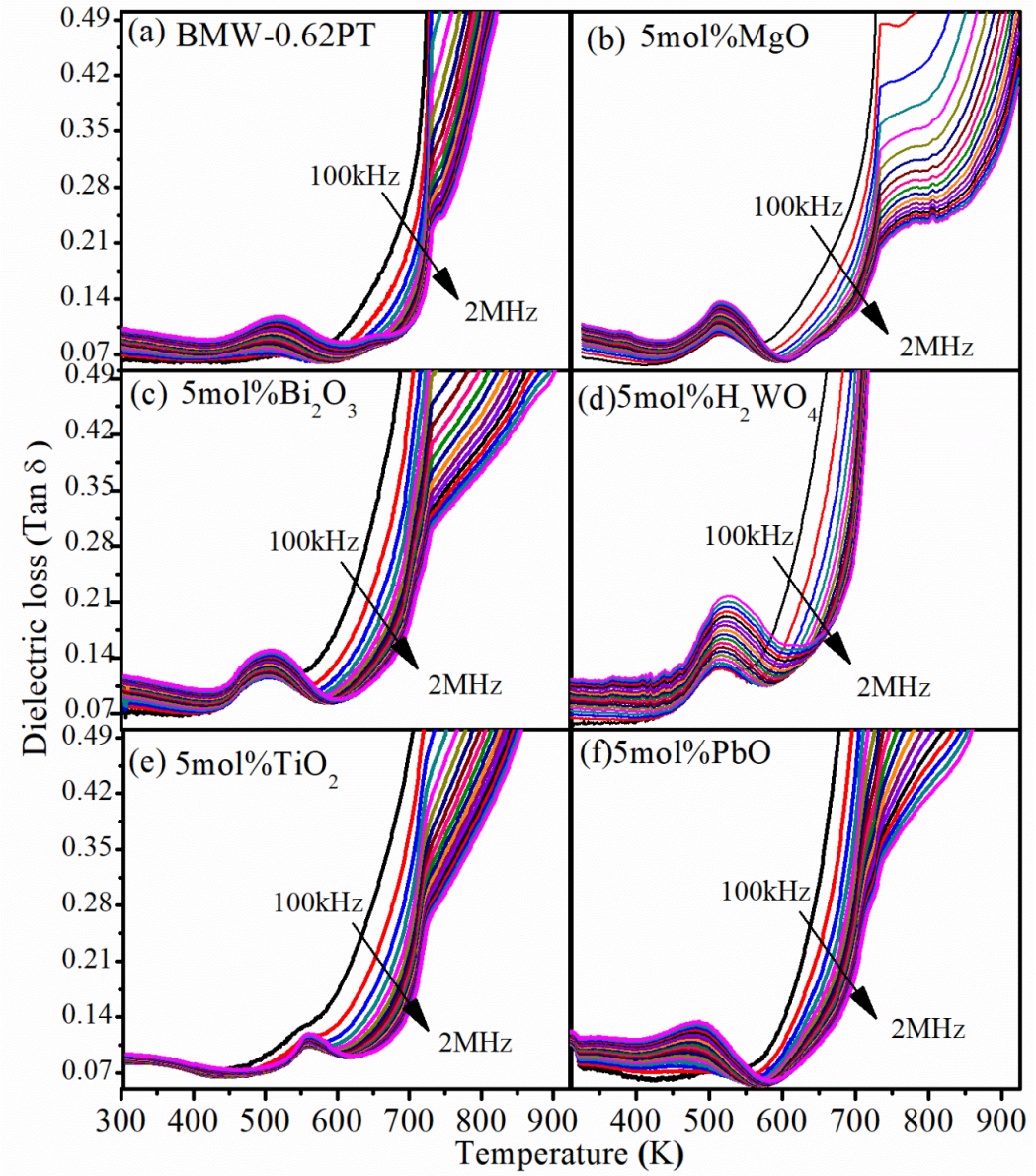


**Figure 4.15** Temperature dependent dielectric loss of 0.38BMW-0.62PT and 5 mol% of (MgO, $Bi_2O_3$, $H_2WO_4$, $TiO_2$ and PbO) at various frequencies.

### 4.4 Conclusions

Crystal structure, microstructure, dielectric and phase transition behaviour of the off-stoichiometric $0.38Bi(Mg_{3/4}W_{1/4})O_3$-$0.62PbTiO_3$ ceramics prepared by adding 1, 2, 3 and 5 mol% of excess PbO, $Bi_2O_3$, MgO, $H_2WO_4$ and $TiO_2$ have been investigated in detail. The Rietveld structure refinement of the off-stoichiometric $0.38Bi(Mg_{3/4}W_{1/4})O_3$-$0.62PbTiO_3$ samples chemically modified with $Bi_2O_3$, MgO, $H_2WO_4$ and $TiO_2$ confirms

the coexistence of cubic (*Fm*-3*m*) and tetragonal (*I*4/*m*) crystal structures similar to stoichiometric sample. The crystal structure of the samples with excess PbO off-stoichiometry exhibit coexisting cubic (*Pm*-3*m*) and tetragonal (*P*4*mm*) phases due to transformation of ordered structure in to disordered structure. All the off-stoichiometric samples exhibit two dielectric anomalies in the temperature dependence of permittivity similar to that for the stoichiometric sample. The temperature dependent dielectric behaviour and dielectric anomaly temperatures are slightly modified by adding excess amount of $Bi_2O_3$, MgO, $H_2WO_4$, PbO and $TiO_2$. The $Bi_2O_3$, MgO and $H_2WO_4$ off-stoichiometry do not result to any significant change in the microstructure. The grain size is significantly increased for the samples with excess PbO while the grain size is significantly decreased in the samples with excess $TiO_2$ in comparison to the grain size of the sintered stoichiometric sample.